

ELECTRONIC SUPPLEMENTARY INFORMATIONS (ESI)

Title: Frequency dependent Energy Storage and Dielectric Performance of Ba-Zr Co-doped BiFeO₃ loaded PVDF based Mechanical Energy harvesters: Effect of Corona Poling

Abhishek Sasmal¹, Shrabanee Sen^{1,*}, P. Sujatha Devi^{1,2,*}

¹Functional Materials and Devices Division, CSIR-Central Glass & Ceramic Research Institute, Kolkata-700032, India

²Chemical Sciences and Technology Division, CSIR-National Institute for Interdisciplinary Science and Technology, Thiruvananthapuram-695019, India

*E-mail: shrabanee@cgcri.res.in, psujathadevi@niist.res.in

ESI: S1

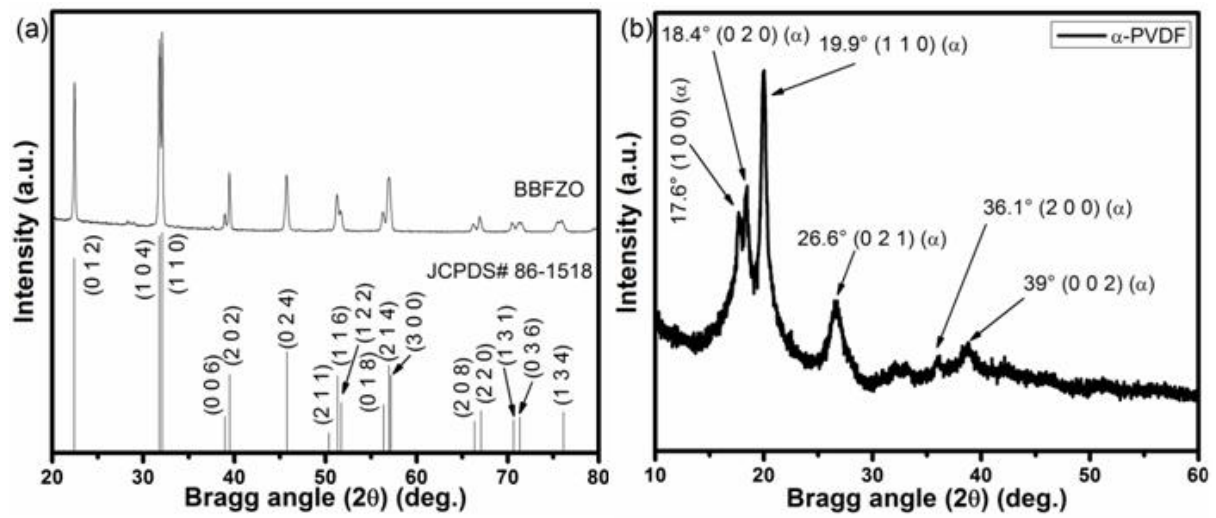


Fig. S1 Indexed XRD pattern of (a) BBFZO nanoparticles and (b) PVDF film.

ESI: S2

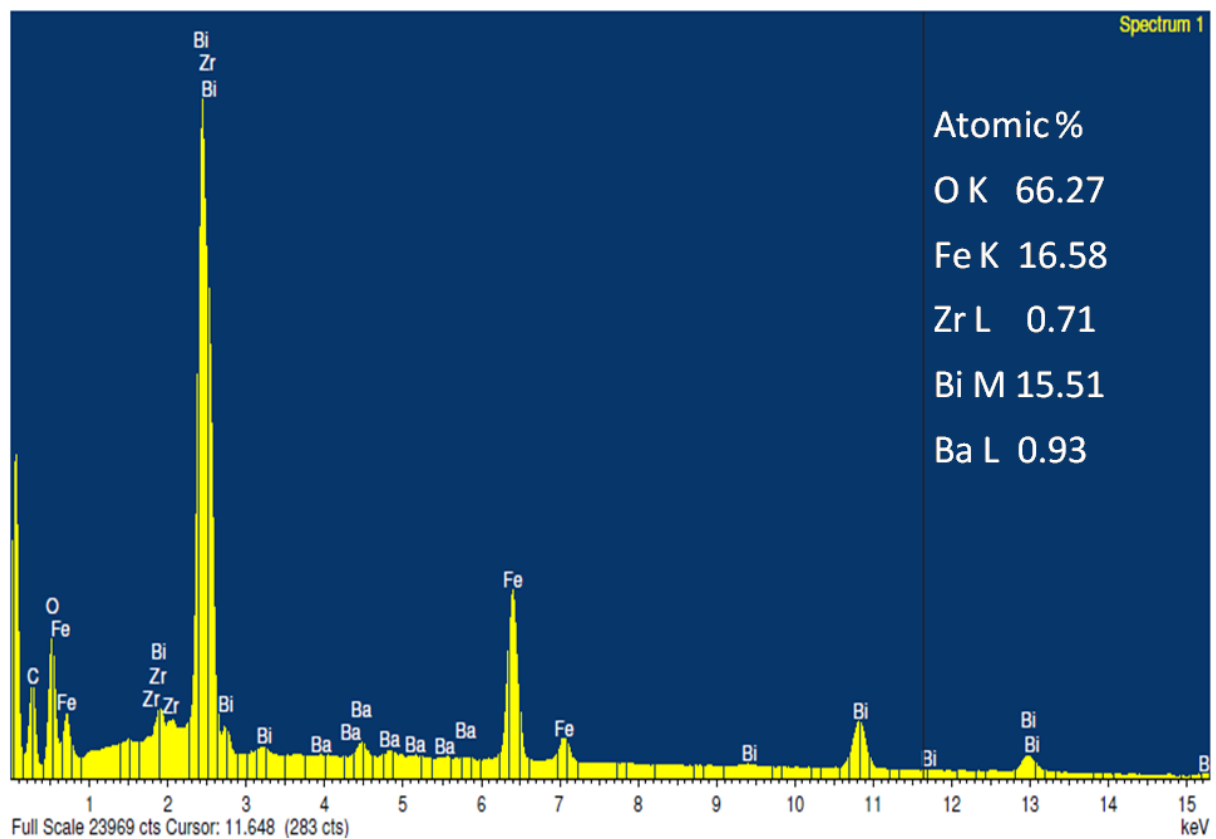


Fig. S2 EDX spectra of BBFZO sample.

ESI: S3

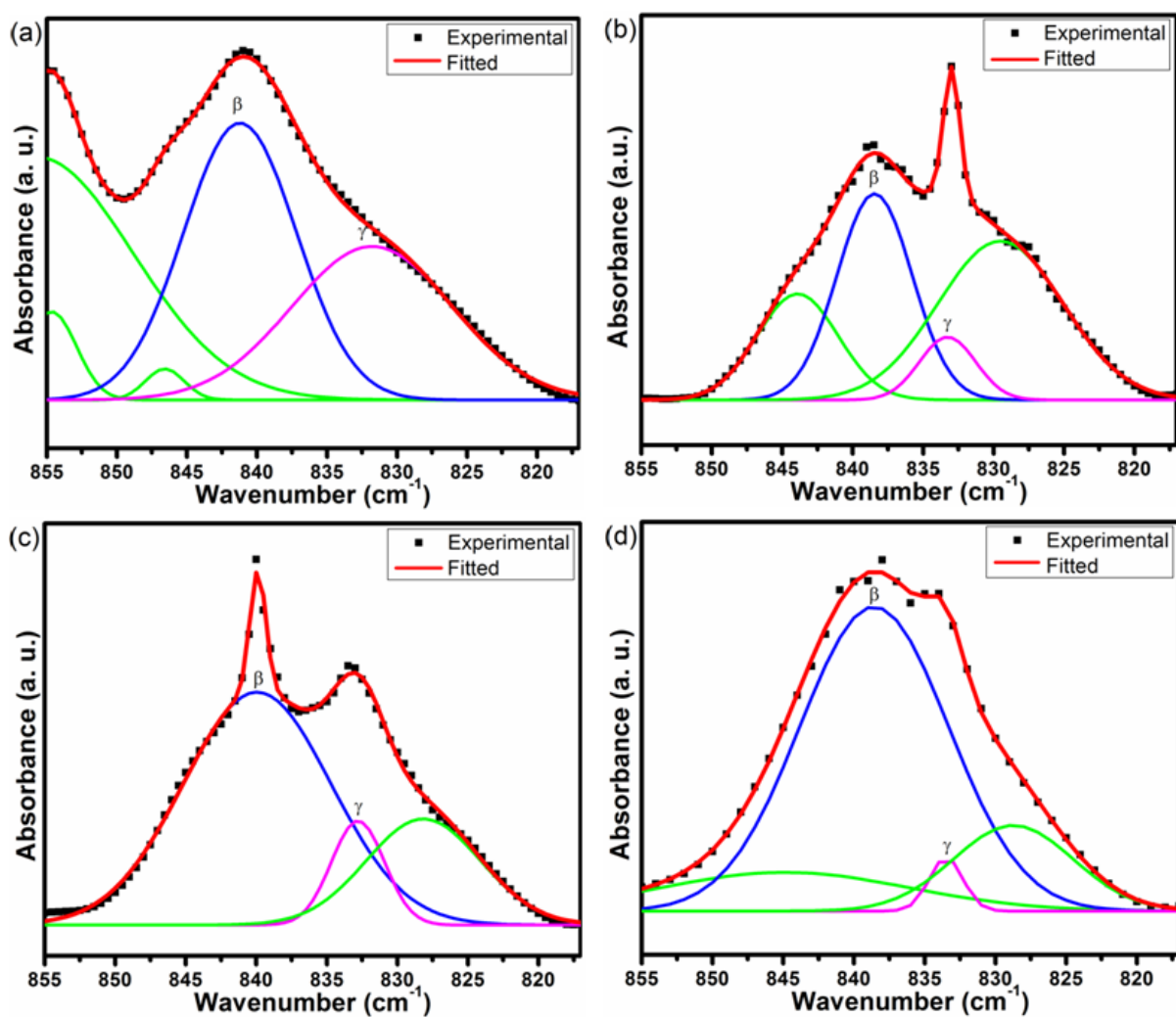


Fig. S3 Deconvoluted FTIR spectra of (a) PVDF, (b) 10BBFZO, (c) 15BBFZO ad (d) Poled-15BBFZO films within the wavenumber range of $855 - 817 \text{ cm}^{-1}$.

ESI: S4

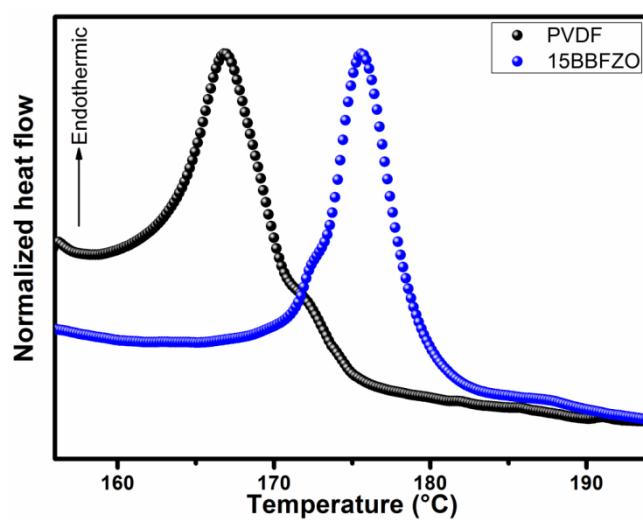


Fig. S4 DSC curves of neat PVDF and 15BBFZO films.

ESI: S5

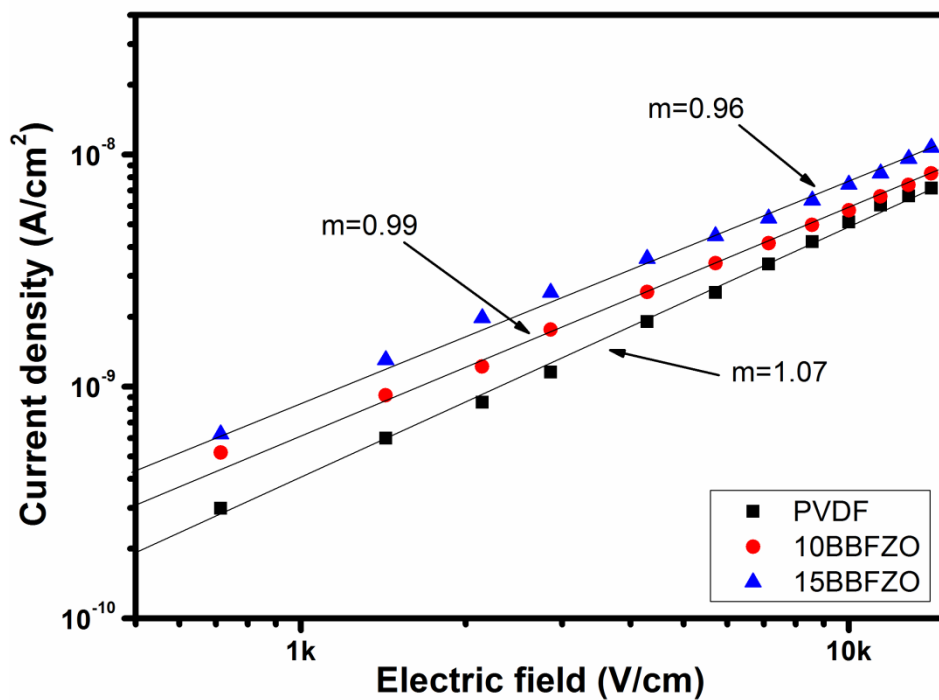


Fig. S5 log J vs. log E graphs for PVDF, 10BBFZO and 15BBFZO films.

ESI: S6

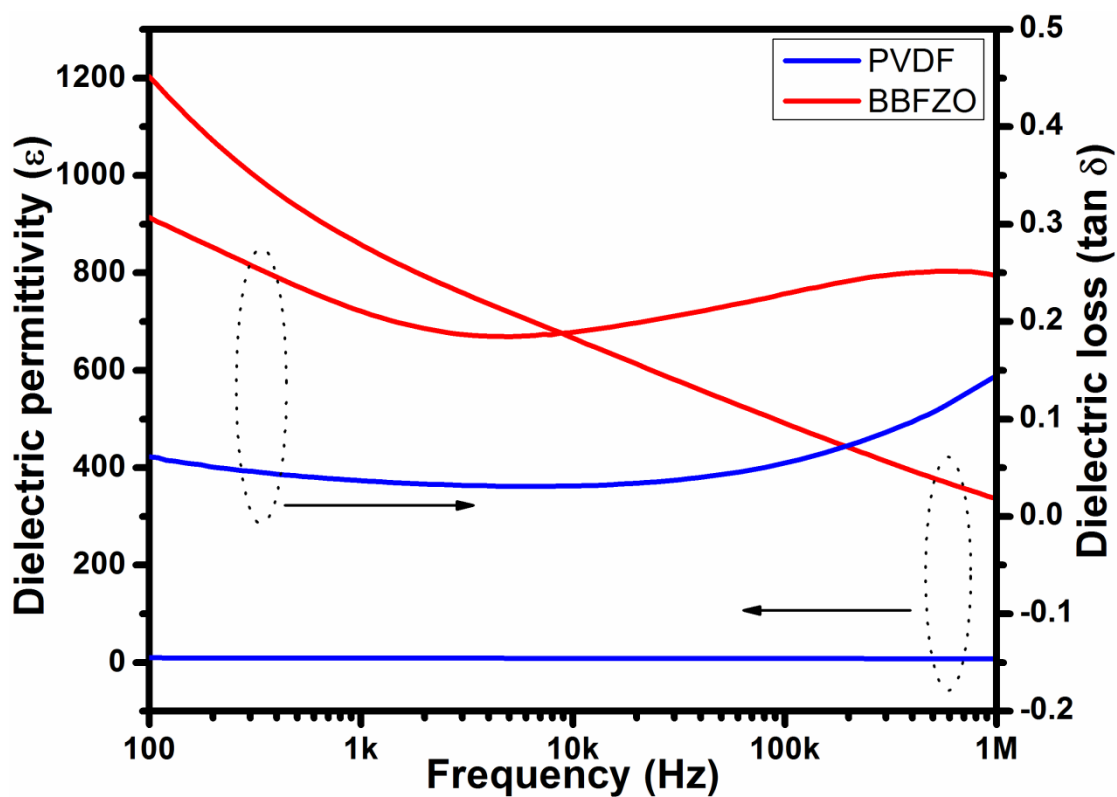


Fig. S6 Dielectric permittivity and $\tan \delta$ of host PVDF matrix and BBFZO filler.

ESI: S7

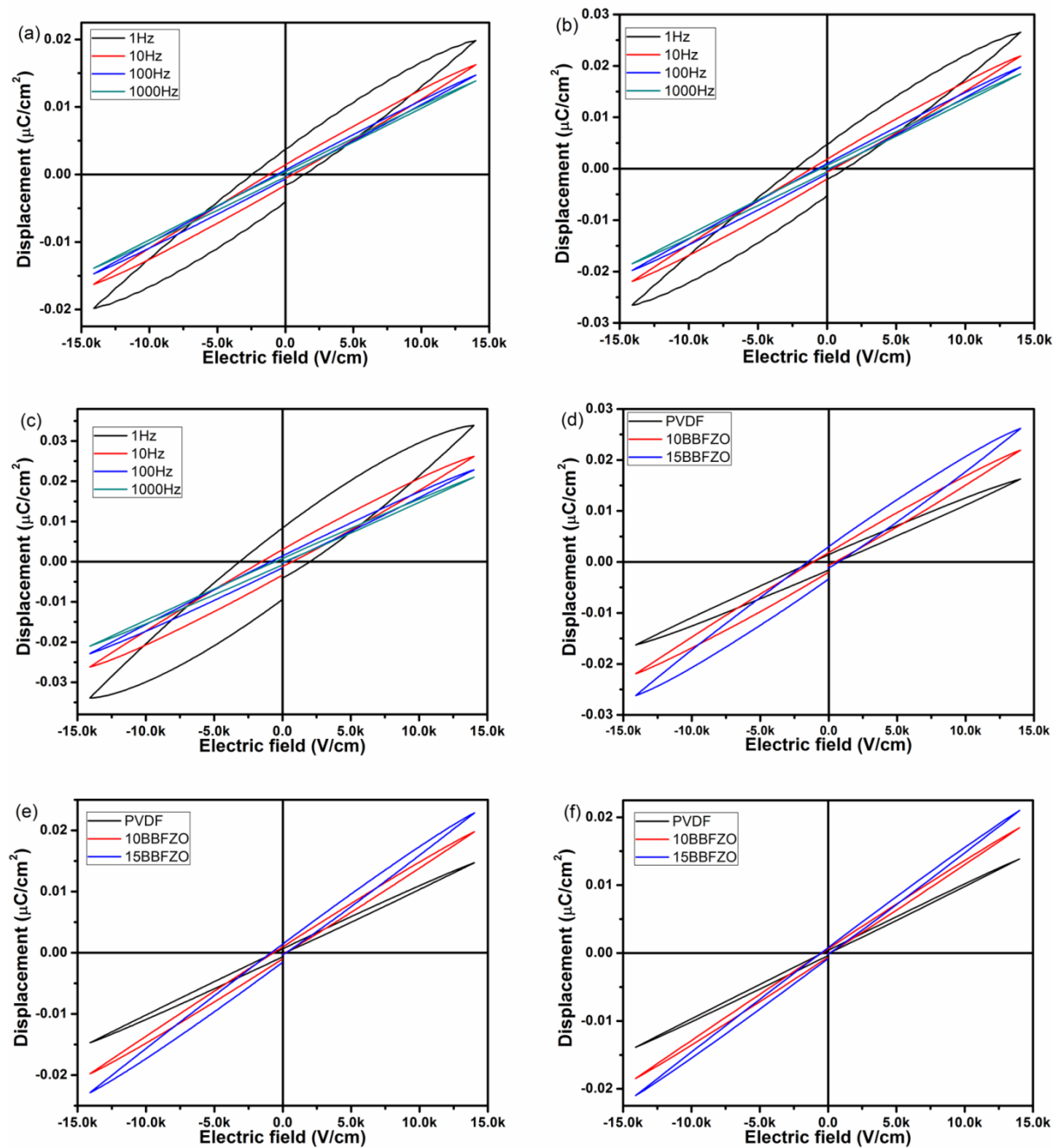


Fig. S7 Comparison of D - E hysteresis loops of (a) PVDF, (b) 10BBFZO and (c) 15BBFZO films at different frequency. Comparison of D - E hysteresis loops of PVDF, 10BBFZO and 15BBFZO films at (d) 10 Hz, (e) 100 Hz and (f) 1000 Hz frequency.

ESI: S8

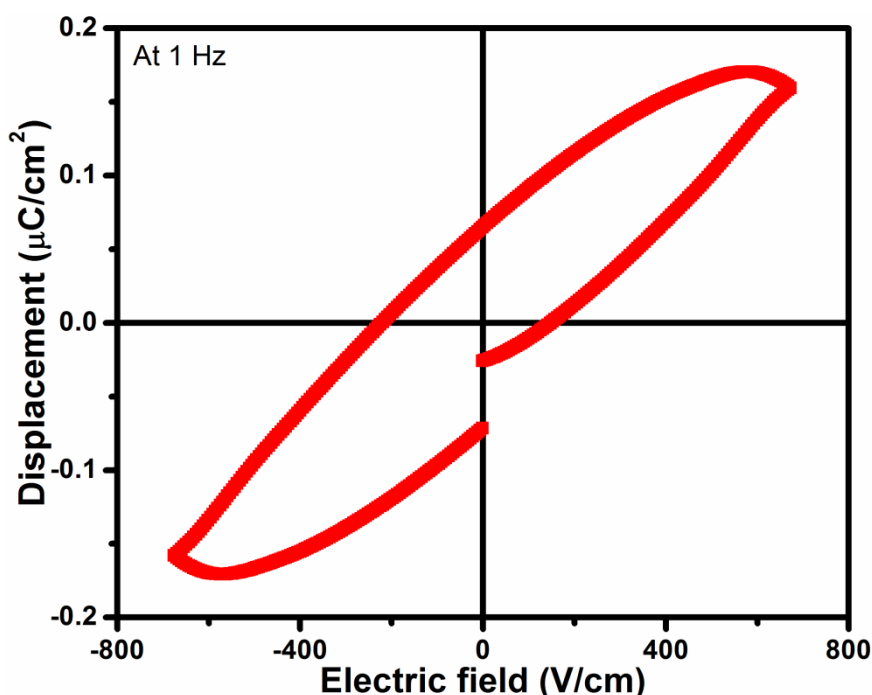


Fig. S8 *D-E* hysteresis loop of ceramic BBFZO filler.

ESI: S9

To optimize the poling condition, extensive study of dielectric permittivity of a composite film at different poling condition was carried out. As the average room temperature was $\sim 35^{\circ}\text{C}$ during the experiment, to avoid the room temperature up-down at different time of the day, slightly higher temperature (40°C) was chosen during all the poling experiments. The optimization of poling field and time of 10BBFZO sample is shown in Fig. S9.

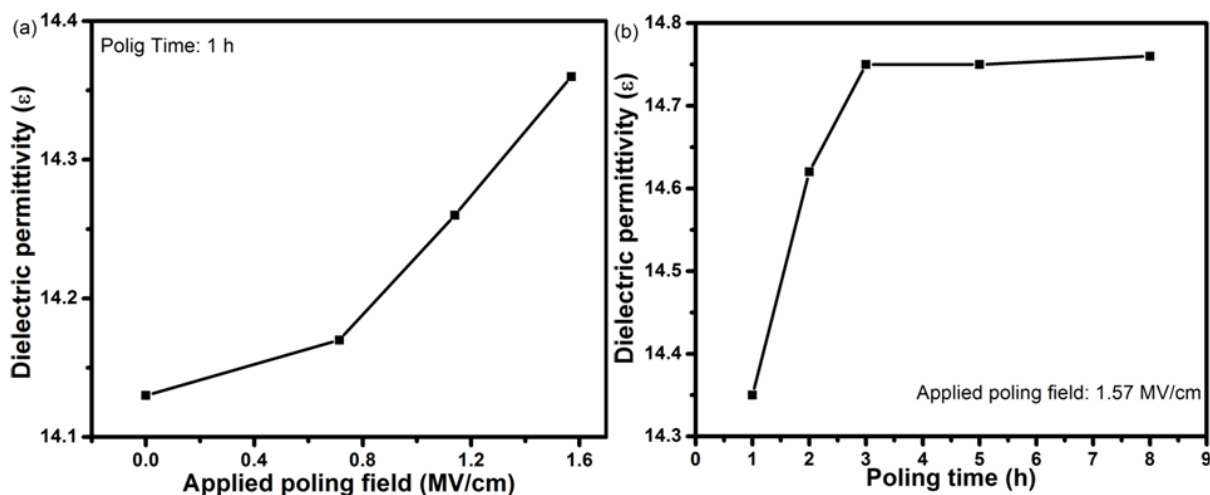


Fig. S9 Variation of dielectric permittivity (a) with the variation of applied field for poling at fixed poling time and (b) with the variation of poling time at fixed applied field for 10BBFZO film.

Though the changes of dielectric permittivity were very little, Fig. S9(a) showed an improvement of permittivity with the increase in applied poling field (at fixed poling time of

1 h). After the applied field of 1.57 MV/cm, breakdown of the composite film occurred. Therefore 1.57 MV/cm was chosen as the optimized poling field. Now to optimize the poling time, the composite film was poled at 1.57 MV/cm field at different poling time. The variation of dielectric permittivity of 10BBFZO with the variation of poling time (at fixed applied field of 1.57 MV/cm) is shown in Fig. S9(b). Dielectric permittivity improved with the increase in poling time up to 3 h. But after 3 h, no significant increase in permittivity (up to 8 h) was observed for the particular composite film. Therefore, the optimized poling time was taken as 3 h. Therefore, the optimized poling condition was chosen as follow.

Optimized poling conditions: Temperature = 40°C, Applied poling field = 1.57 MV/cm, Poling time = 3 h.

Variation of poling temperature was not studied here because we tried to perform all the experiments around room temperature.

ESI: S10

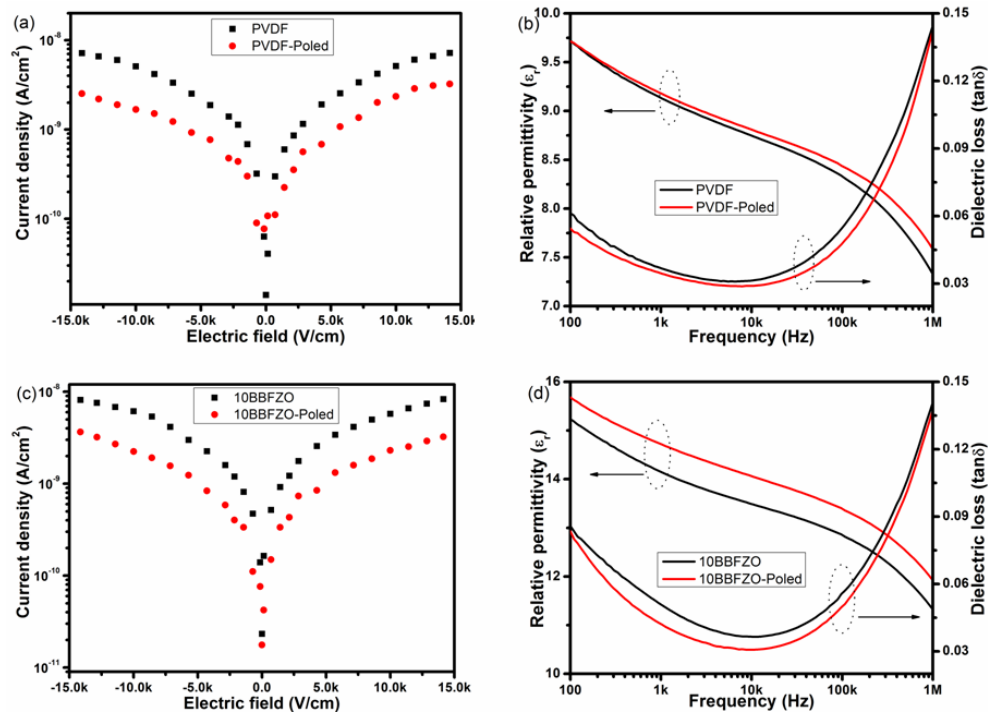


Fig. S10 (a) Leakage current density and (b) dielectric property of unpoled and poled PVDF. (c) Leakage current density and (d) dielectric property of unpoled and poled 10BBFZO.

ESI: S11

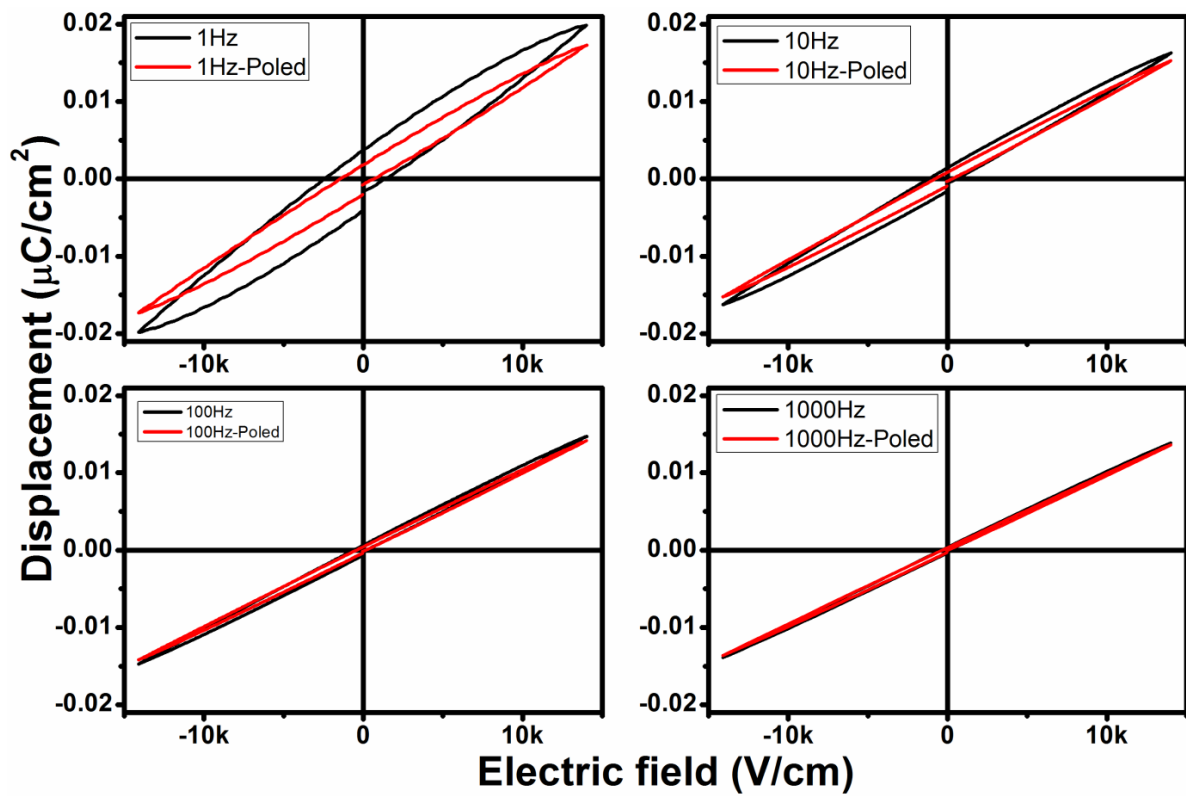


Fig. S11 *D-E* hysteresis loops of unpoled and poled PVDF at different frequency.

ESI: S12

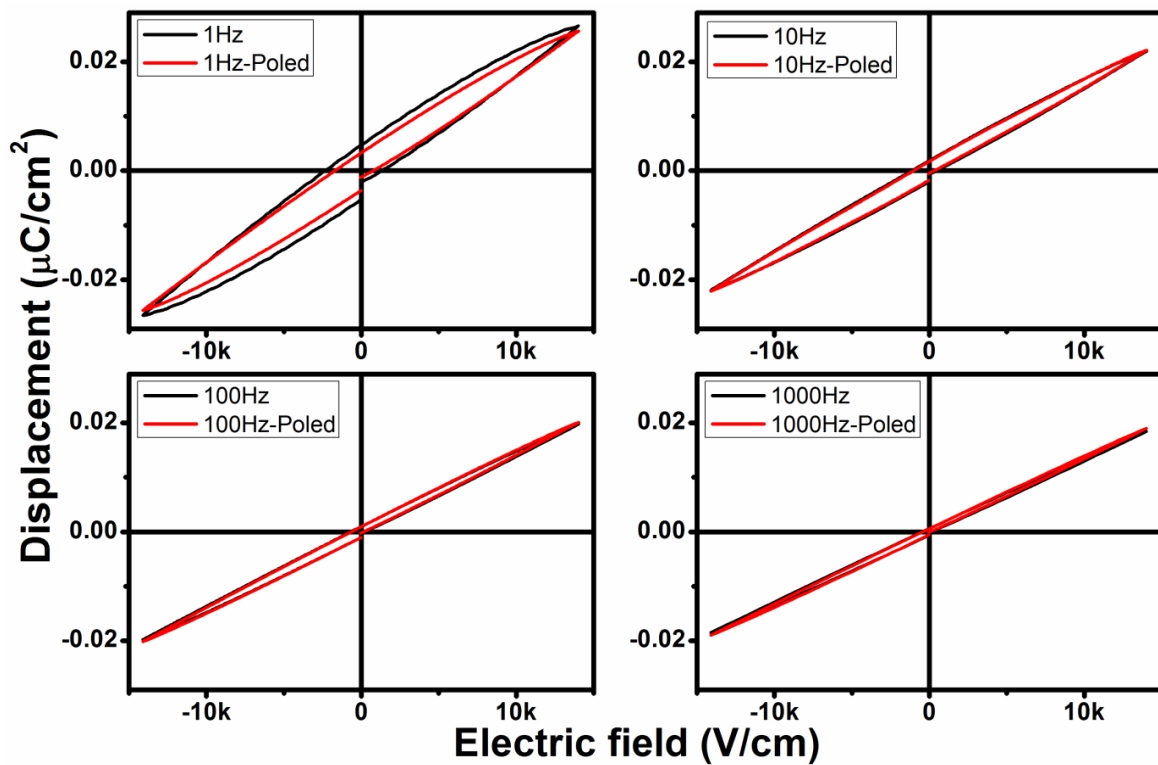


Fig. S12 *D-E* hysteresis loops of unpoled and poled 10BBFZO at different frequency.

ESI: S13

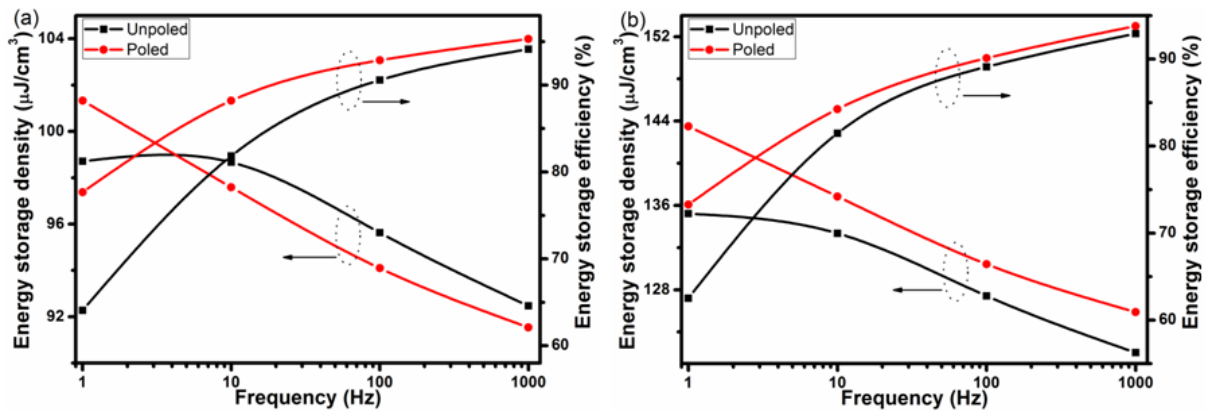


Fig. S13 Frequency dependent energy storage density and storage efficiency of unpoled and poled (a) PVDF and (b) 10BBFZO films.